

UC San Diego

UC San Diego Previously Published Works

Title

An infrared probe of tunable dielectrics in metal-oxide-semiconductor structures

Permalink

<https://escholarship.org/uc/item/8ff9r9xh>

Journal

Applied Physics Letters, 86(22)

ISSN

0003-6951

Authors

Li, Z Q
Wang, G M
Mikolaitis, K J
[et al.](#)

Publication Date

2005-05-01

Peer reviewed

An infrared probe of tunable dielectrics in metal-oxide-semiconductor structures

Z. Q. Li^{a)}

Department of Physics, University of California, San Diego, La Jolla, California 92093

G. M. Wang

Institute for Polymers and Organic Solids, University of California, Santa Barbara, Santa Barbara, California 93106

K. J. Mikolaitis

Department of Physics, University of California, San Diego, La Jolla, California 92093

D. Moses and A. J. Heeger

Institute for Polymers and Organic Solids, University of California, Santa Barbara, Santa Barbara, California 93106

D. N. Basov

Department of Physics, University of California, San Diego, La Jolla, California 92093

(Received 9 November 2004; accepted 6 May 2005; published online 26 May 2005)

A composite metal-polymer electrode is designed to investigate electric-field-induced changes of the dielectric function of gate insulators in metal-oxide-semiconductor structures using infrared spectroscopy. We studied structures based on TiO₂ dielectric insulator on doped silicon, a combination commonly used in field-effect transistors. It is shown that the voltage-induced changes of the dielectric constant in TiO₂ originate from a modification of the lattice vibration modes of this compound. © 2005 American Institute of Physics. [DOI: 10.1063/1.1942645]

High dielectric constant [$\epsilon_1(0)$] insulators have the potential to serve as alternative gate dielectric materials in metal-oxide-semiconductor (MOS) structures to circumvent the fundamental scaling limitations of SiO₂.¹ Because enhanced values of $\epsilon_1(0)$ in oxides stem from their giant ionic polarizabilities, these systems are inherently susceptible to applied electric fields.^{2,3} It is therefore prudent to characterize field-induced modifications of $\epsilon_1(0)$ under operational conditions in realistic MOS devices. Conventional spectroscopic investigations of MOS structures usually utilize ultrathin semitransparent metallic electrodes.^{4,5} However, in these earlier works, experiments in the far-infrared were prohibitively difficult because of the poor transparency of the metallic electrodes.⁶ Here we report on an electrode comprised of interdigitated Au contacts covered with a polymer film that is ideally suited for the study of electric field induced effects in the far-IR and applied this electrode to investigate field-induced changes of $\epsilon_1(\omega \rightarrow 0)$ in TiO₂ incorporated in a MOS structure. We show that the origin of voltage-induced changes of $\epsilon_1(0)$ is the hardening of IR-active phonons in TiO₂.

An example of the MOS structure explored in this work is displayed in the left panel of Fig. 1. In these structures a 180 nm layer of TiO₂ is deposited on a 500 μm *n*-doped Si substrate that also serves as the gate electrode. A 6 nm SiO₂ layer is deposited onto the TiO₂ layer.⁷ Interdigitated source and drain gold contacts form a grid on the insulating layer with the grid spacing ranging from 50 to 200 μm . Contacts for standard four-probe measurements are also deposited, enabling monitoring of the *I*-*V* characteristics of the particular device employed for the spectroscopic study. The final stage of the device fabrication is coating with a 4 nm thin film of

poly(3-hexylthiophene) (P3HT). Charge injection into the accumulation layer in the polymer film⁸ allows one to maintain an electric field in the region between the thick Au grids, a virtue not offered by ordinary interdigitated electrodes. Because the polymer film is highly transparent even under charge injection, these large-area (>1 cm²) “grid-electrode” structures offer significant advantages over conventional approaches⁴⁻⁶ to study the modifications of optical properties by applied electric field. Here we will focus on the analysis of voltage-induced modifications of TiO₂ in the far-IR region facilitated by grid-electrode structures; spectroscopic studies of the effects of applied electric field on the polymer will be reported separately.

In Fig. 2 we summarize our results for a representative composite electrode device. The top panel shows the ratios of transmission spectra at different voltages applied between the Si substrate and Au grid-electrodes normalized by transmission at $V=0$: $T(\omega, V)/T(\omega, 0)$. All spectra were measured at room temperature with unpolarized light, with a spectral

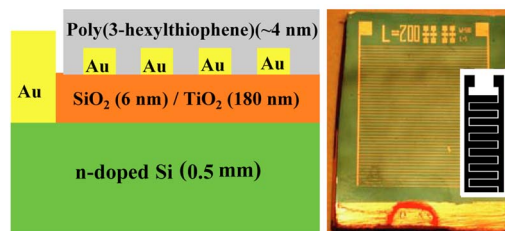


FIG. 1. (Color online) Left panel: a schematic of the MOS device with a composite metal-polymer top electrode. Right panel: a photograph of the actual device along with a schematic representation of the electrodes. The Au bar at the bottom of the structure is a contact to the substrate. The contacts on the top of the structure are intended for four-probe measurements of *I*-*V* characteristics.

^{a)}Electronic mail: zhiqiang@physics.ucsd.edu

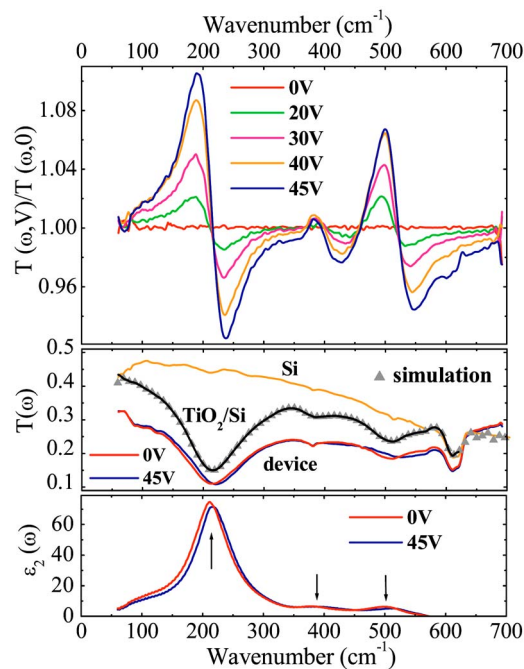


FIG. 2. (Color online) Top panel: the ratios of transmission spectra of a device with a grid spacing of $50 \mu\text{m}$ at different applied voltages between the Si substrate and Au grid-electrodes. The same potential was applied to the source and drain, therefore, the source-drain current was zero. Middle panel: the transmission spectrum of the Si substrate and the TiO_2/Si bilayer. With the carrier concentration in the n -Si in the 10^{18}cm^{-3} range, the substrate and therefore the entire device shows relatively high transmission $T(\omega) \approx 20\% - 50\%$ in the far-IR region. A fit of $T(\omega)$ for the TiO_2/Si bilayer using a Kramers-Kronig constrained algorithm is represented by gray triangles, $T(\omega)$ of the device at 0 V (red line), and 45 V (blue line). Bottom panel: $\epsilon_2(\omega)$ of the TiO_2 film at zero applied voltage and 45 V extracted from the KK constrained fitting. The three absorptions peaks (marked by arrows) in $\epsilon_2(\omega)$ are due to the TO modes of the TiO_2 film. Under applied field, the TO frequencies harden, as evident from both transmission data and $\epsilon_2(\omega)$ spectra.

resolution of 1cm^{-1} . The middle panel displays the absolute transmission of the device at zero applied voltage and at $V = 45 \text{V}$. The dips in the $T(\omega)$ spectra of the device at 216, 386, and 503cm^{-1} are due to absorptions associated with the TO phonon modes of TiO_2 .^{9,10} When a biasing voltage is applied to the device, these modes harden (middle panel of Fig. 2) leading to strong resonances in the $T(\omega, V)/T(\omega, 0)$ spectra. Transmission changes reach 10% near 200cm^{-1} at 45 V, a voltage close to the breakdown threshold of these devices. A reference structure without a polymer film did not show appreciable changes in $T(\omega)$ suggesting that the effect is intimately related to the presence of the electric field between the Au contacts. Indeed, under the applied voltage, the $\text{SiO}_2/\text{TiO}_2$ bilayer is effectively placed in a capacitor formed by charge-injected polymer at the top and n -Si substrate at the bottom. Note that the Au grid electrodes are not transpar-

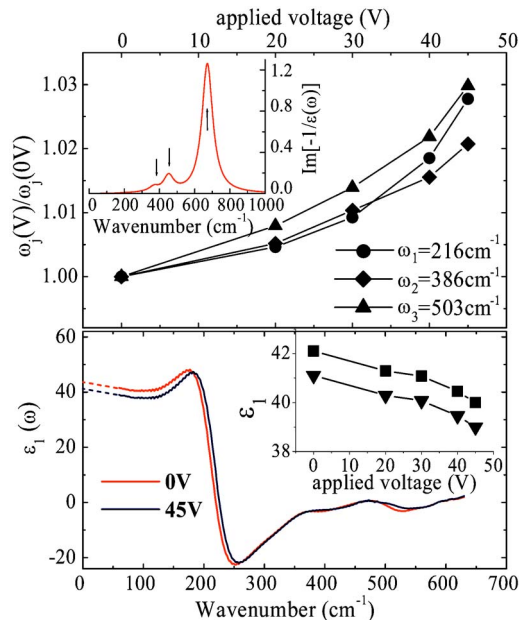


FIG. 3. (Color online) The loss function $\text{Im}[-1/\epsilon(\omega)]$ (top inset) and the real part of the dielectric function $\epsilon_1(\omega)$ (bottom panel) of the TiO_2 film obtained from the KK constrained fitting of the transmission spectra. The peaks marked by arrows in top inset are the LO modes of the TiO_2 film. The dashed lines below 60cm^{-1} are extrapolations of $\epsilon_1(\omega)$ to zero frequency. Top panel: the ratios of TO phonon frequencies of the TiO_2 film with and without applied voltage from Table I. Bottom inset: ϵ_1 at 60cm^{-1} (solid triangle) and zero frequency extrapolation $\epsilon_1(\omega \rightarrow 0)$ (solid square) of the TiO_2 film at different applied voltages. Under applied voltage the phonon resonances harden, whereas the absolute value of the static dielectric constant is reduced.

ent in the far-IR region. Therefore, the field-induced changes of optical properties of the sample are produced primarily by the polymer and $\text{SiO}_2/\text{TiO}_2$ in regions between the Au bars.

In order to quantify the field-induced modifications of the IR response of TiO_2 it is imperative to evaluate the optical constants of all layers constituting our P3HT/ $\text{SiO}_2/\text{TiO}_2/n$ -Si devices. The complex dielectric function of the n -Si substrate $\epsilon^{\text{Si}}(\omega)$ was determined from a combination of transmission $T(\omega)$ and reflectance $R(\omega)$ measurements.¹¹ Next, we measured $T(\omega)$ spectra for a TiO_2/n -Si bilayer. The complex dielectric function of TiO_2 $\hat{\epsilon}^{\text{TiO}_2}(\omega) = \epsilon_1^{\text{TiO}_2}(\omega) + i\epsilon_2^{\text{TiO}_2}(\omega)$ was then evaluated from these measurements using a Kramers-Kronig (KK) constrained fitting algorithm¹² by properly including multiple reflections occurring in the TiO_2/n -Si bilayer. Within the absolute uncertainty of our measurements (0.5%), the 6 nm layer of SiO_2 did not produce a noticeable effect on the $T(\omega)$ of the device and was ignored in the analysis. We have verified that the absorption associated with the accumulation layer in P3HT and in n -Si has no impact on the $T(\omega)$ spectra in the

TABLE I. The TO and LO frequencies of the j th phonon mode ($\omega_{\text{TO}j}$ and $\omega_{\text{LO}j}$, in cm^{-1}) of the TiO_2 film at 0 and 45 V and those of bulk TiO_2 with rutile structure. The uncertainty of the TO frequencies is 1cm^{-1} (our spectral resolution) and that of the LO frequencies is less than 10cm^{-1} (the uncertainty of our simulation).

	$\omega_{\text{TO}1}$	$\omega_{\text{TO}2}$	$\omega_{\text{TO}3}$	$\omega_{\text{LO}1}$	$\omega_{\text{LO}2}$	$\omega_{\text{LO}3}$
TiO_2 film	216	386	503	672	376	453
TiO_2 film (45 V)	222	394	518	680	379	466
Bulk TiO_2 (rutile) ^a	183	388	500	807	373	458

^aReference 9.

frequency region of TiO₂ phonons.¹³ Therefore, it is unnecessary to account for the response of accumulation layers in the analysis. As expected, the primary effect of the gold grid is to reduce the absolute value of the $T(\omega)$ of the device without introducing new features to $T(\omega)$ in the frequency range of interest, where the phonon modes of TiO₂ dominate the IR response (middle panel of Fig. 2).

The dielectric function of the TiO₂ layer (Figs. 2 and 3) extracted from the analysis detailed above displays three resonances that can be described with the usual Lorentzian form

$$\epsilon(\omega) = \epsilon_\infty + \sum_j \frac{\omega_{pj}^2}{\omega_{0j}^2 - \omega^2 - i\gamma_j\omega}, \quad (1)$$

where γ_j and ω_{pj} are the linewidth and plasma frequency of the j th mode at ω_{0j} , respectively. Field-induced hardening of TO modes of TiO₂ evident in the raw $T(\omega)$ data for our devices is also clearly seen in the spectra of the real and imaginary parts of the dielectric function of the TiO₂ layer. All three TO modes harden by approximately 3% at 45 V (Fig. 3). Frequencies for the LO modes of TiO₂ can be obtained from Eq. (1) using the relationship $\omega_{LOj}^2 = \omega_{TOj}^2 + \omega_{pj}^2$. The TO and LO phonon modes for both the TiO₂ film and bulk TiO₂ with rutile structure⁹ are listed in Table I. The modification of the lattice dynamics of TiO₂ by applied electric field is not unexpected since TiO₂ is an incipient ferroelectric.¹⁴ Indeed, field-induced changes of the static dielectric constant $\epsilon_1(0)$ have been previously reported for other ferroelectrics.^{15,16} The real part of the dielectric function $\epsilon_1(\omega)$ of TiO₂ gate insulator is plotted in the bottom panel of Fig. 3. The bottom inset of Fig. 3 also displays the voltage dependence of $\epsilon_1(\omega=60 \text{ cm}^{-1})$ along with the zero frequency extrapolation of $\epsilon_1(\omega)$, which is a reliable estimate of $\epsilon_1(0)$. The $\epsilon_1(0)$ of TiO₂ film obtained from our infrared measurements (~ 42) is consistent with capacitive measurements (~ 41).⁷ However, both of these results are significantly smaller than the bulk value reported for crystalline TiO₂ (~ 90).¹⁴

Insights into the reduction of $\epsilon_1(0)$ in films compared to that of bulk crystals and into its field-induced modification are provided by the Lyddane-Sachs-Teller (LST) relation¹⁷

$$\frac{\epsilon_1(0)}{\epsilon_\infty} = \prod_{j=1}^N \frac{\omega_{LOj}^2}{\omega_{TOj}^2}. \quad (2)$$

The relation connects $\epsilon_1(0)$ and the high-frequency dielectric constant ϵ_∞ to the frequencies of LO and TO phonon modes of a crystal (ω_{LOj} and ω_{TOj} , respectively). Using the values in Table I together with $\epsilon_\infty \sim 6.84$ for rutile¹⁸ and $\epsilon_\infty \sim 5$ for the TiO₂ thin film from our modeling, we obtain $\epsilon_1(0) \sim 103$ for the crystal and $\epsilon_1(0) \sim 37$ for the TiO₂ film from Eq. (2). Therefore, the reduction of $\epsilon_1(0)$ in the film is a consequence of smaller TO-LO splitting compared to that of a bulk mate-

rial. The field-induced changes of $\epsilon_1(0)$ are also consistent with the LST relation. Indeed, the voltage-induced hardening of the TO modes fully accounts for the reduction of $\epsilon_1(0)$ by about 3% (as shown in the bottom inset of Fig. 3). Our measurements demonstrate that *all* TO modes of the TiO₂ film are modified by the applied electric field. This finding is in accord with Cochran's theory of ferroelectricity,² where all nonlinear terms in the short-range forces are equally important. An interconnection between the field-induced modification of phonon frequencies and the reduction of $\epsilon_1(0)$ reported here affords adjustable dielectric characteristics widely employed in tunable microwave devices.³

In conclusion, we show that a composite metal-polymer electrode enables far-IR spectroscopic characterization of gate insulators exploited in the MOS architecture. Our results reveal that the microscopic origins of tunable dielectric response of the TiO₂ gate insulator are associated with the hardening of TO phonons in applied electric fields. The characterization capabilities documented here uncover the unique potential of infrared spectroscopy for the analysis of tunable insulators and also for examination of charge injection phenomena in semiconductors.

Work at UCSD is supported by NSF and PRF.

¹G. D. Wilk, R. M. Wallace, and J. M. Anthony, *J. Appl. Phys.* **89**, 5243 (2001).

²W. Cochran, *Adv. Phys.* **9**, 387 (1960).

³A. K. Tagantsev, V. O. Sherman, K. F. Astafiev, J. Venkatesh, and N. Setter, *J. Electroceram.* **11**, 5 (2003).

⁴M. G. Harrison, D. Fichou, F. Garnier, and A. Yassar, *Opt. Mater.* **9**, 53 (1998).

⁵P. J. Brown, H. Siringhaus, M. Harrison, M. Shkunov, and R. H. Friend, *Phys. Rev. B* **63**, 125204 (2001).

⁶K. E. Ziemelis, A. T. Hussain, D. D. C. Bradley, R. H. Friend, J. Rühle, and G. Wegner, *Phys. Rev. Lett.* **66**, 2231 (1991).

⁷G. Wang, D. Moses, A. J. Heeger, H.-M. Zhang, Mux Narasimhan, and R. E. Demaray, *J. Appl. Phys.* **95**, 316 (2004). The SiO₂/TiO₂ bilayer significantly improves the characteristics of P3HT-based FET device compared to a single layer of TiO₂.

⁸L. Burgi, H. Siringhaus, and R. H. Friend, *Appl. Phys. Lett.* **82**, 1482 (2003).

⁹C. Lee, P. Ghosez, and X. Gonze, *Phys. Rev. B* **50**, 13379 (1994).

¹⁰M. Mikami, S. Nakamura, O. Kitao, and H. Arakawa, *Phys. Rev. B* **66**, 155213 (2002). Small discrepancies with the TO modes in bulk TiO₂ presumably originate from polycrystalline nature of the films and/or from stress in the film due to lattice mismatch between *n*-Si and TiO₂.

¹¹See, for example, E. J. Singley, K. S. Burch, R. Kawakami, J. Stephens, D. D. Awschalom, and D. N. Basov, *Phys. Rev. B* **68**, 165204 (2003).

¹²A. Kuzmenko (unpublished); computer code is available at <http://optics.unige.ch/alexey/reffit.html>

¹³Z. Q. Li, G. M. Wang, A. J. Heeger, and D. N. Basov (unpublished).

¹⁴See for example: G. A. Samara and P. S. Peercy, *Phys. Rev. B* **7**, 1131 (1973), and references therein.

¹⁵P. A. Fleury and J. M. Worlock, *Phys. Rev.* **174**, 613 (1968).

¹⁶I. A. Akimov, A. A. Sirenko, A. M. Clark, J.-H. Hao, and X. X. Xi, *Phys. Rev. Lett.* **84**, 4625 (2000).

¹⁷R. H. Lyddane, R. G. Sachs, and E. Teller, *Phys. Rev.* **59**, 673 (1941).

¹⁸J. G. Traylor, H. G. Smith, R. M. Nicklow, and M. K. Wilkinson, *Phys. Rev. B* **3**, 3457 (1971).